CIENCIA 19(1), 50 - 65, 2011
Maracaibo, Venezuela

Visualization of convective plasma cells in 2D

*Rodrigo Carboni and Francisco Frutos-Alfaro**
Space Research Center (CINESPA) and School of Physics, University of Costa Rica.
San José, Costa Rica

Abstract

Computer simulations of plasmas are relevant nowadays, because it helps us understand physical processes taking place in the sun and other stellar objects. We developed a program, called XPCell, which is intended for displaying the evolution of the magnetic field in a 2D convective plasma cell with perfect conducting walls for different stationary plasma velocity fields. Applications of this program are presented. This software works interactively with the mouse via a graphical user interface. XPCell graphical user interface was generated with XForms. For displaying the simulations, XPCell uses free version of OpenGL, which is available for all computer systems. This software allows the user to create movies in MPEG and AVI format.

Key words: plasma physics, computer simulations, scientific visualization.

Visualización de celdas de plasma convectivo en 2D

Resumen

Las simulaciones por ordenador de los plasmas son relevantes hoy en día, porque nos ayudan a comprender los procesos físicos que tienen lugar en el sol y otros objetos estelares. Hemos desarrollado un programa, llamado XPCell, que está diseñado para mostrar la evolución del campo magnético en una celda convectiva del plasma en 2D con paredes perfectamente conductoras para diferentes campos de velocidades estacionarios del plasma. Las aplicaciones de este programa se presentan en este artículo. Este software funciona interactivamente con el ratón a través de una interfaz gráfica de usuario. La interfaz gráfica de usuario XPCell se ha generado con XForms. Para visualizar las simulaciones, XPCell utiliza la versión gratuita de OpenGL, que está disponible para todos los sistemas operativos. Este software permite al usuario crear películas en formato MPEG y AVI.

Palabras clave: física de plasmas, simulaciones por computadora, visualización científica.

1. Introduction

The great advance in computer technology makes possible to simulate and visualize complex physical phenomena taking place in stellar objects, for instance, the convective cells on the sun.

Over the past 50 years, important development have occurred in the intriguing field of magnetohydrodynamics, which describes the generation and persistence of magnetic fields in cosmic sources that take their energy from fluid mechanical energy. Currently, the magnetic field intensity of most celestial bodies and regions of the universe are known; they range from 10^{-9} G in the intergalactic plasma to 10^{12} G at the surface of neutron stars (1).

* To whom mail should be addressed: frutos@fisica.ucr.ac.cr

The approach most researchers use to understand this dynamo mechanism is to consider a cosmic plasma with a stationary motion, which leads to an induction problem where the goal is to find stationary states as solutions of the induction equation. Nowadays, this kind of equation is easily solved via computer. W. M. Elssaser, N. O. Weiss, and E. N. Parker performed the first two-dimensional simulations (2-4). More recent simulations by Weiss (1975), P. A. Galloway include dynamical effects and are generalized to three dimensions for the kinematic case (5-7). In recent years dynamo models have been improved by considering fully dynamical solutions of the induction equation taking into account the coupled mass, momentum and energy relations for the plasma. Recently P. D. Mininni *et al.* have considered the Hall current into the dynamo model (8).

We can simulate convection cells by choosing convective velocity fields, which in turn help us understand the behavior of granules, mesogranules in the photosphere, supergranules in the photosphere and chromosphere, and laboratory plasmas. We also can investigate the not-well-understood phenomena of reconnection in this way (9).

The XPCell program helps visualize the magnetic field's evolution in different convective plasmas. We wrote the program in C. The graphical user interface was designed using XFORMS (toolkit) and OpenGL (graphic library). The user can create movies with XPCell. This program runs on Linux or Unix. To get the program, the interested user may visit our website: http://www.cinespa.ucr.ac.cr/software/xpcell/index.html

Pcell (10, 11), the old version is still available. In PCell, the simulation is displayed with GNUPLOT, which is common in all Linux operating systems. The capability to create movies in MPEG format is possible with PCell. The graphical user interface of both programs is basically the same.

2. The Induction Equation

2.1. Conditions

We can obtained the induction equation under certain special conditions:

- The plasma is assumed to be an isotropic, homogeneous medium of constant conductivity σ.
- The effects produced by temperature gradient and density fluctuations of charged particles are neglected.
- The velocity of the charged particles (mechanical velocities) are considered much slower than the electromagnetic field velocity, meaning the relativistic effects are not present.
- The magnetic energy dominates over the electric energy, which means that the force is mainly magnetic.
- The ratio of the convection current or displacement current to the conduction current is very small.

2.2. Deduction of the induction equation

Maxwell's Equations determine electromagnetic fields behavior in a cosmic fluid

$$\begin{aligned} \varepsilon \nabla \cdot \mathbf{E} &= \rho_E , \\ \nabla \times \mathbf{E} &= -\frac{\partial \mathbf{B}}{\partial t}, \\ \nabla \cdot \mathbf{B} &= 0, \\ \nabla \times \mathbf{B} &= \mu\left[\mathbf{J} + \varepsilon \frac{\partial \mathbf{E}}{\partial t}\right], \end{aligned} \qquad [1]$$

where ε is the medium electric permittivity, μ is the medium magnetic permeability, ρ_E is the charged particles density and $\mathbf{J}$ is the current density. The effects produced by the temperature gradient and charged particles density fluctuations had been neglected.

The general expression for the current density $\mathbf{J}$ in an isotropic homogeneous medium is:

$$\mathbf{J} = \sigma[\mathbf{E} + \mathbf{v} \times \mathbf{B}] + \rho_E \mathbf{v}, \quad [2]$$

where the right-hand-side terms are the conduction, induction and convection currents respectively. The conductivity σ is considered constant in the whole plasma and $\mathbf{v}$ is the velocity field that describes the plasma motion.

We can simplify the above equations by comparing the orders of magnitude of the quantities involved. We represent orders of magnitude with square brackets. In cosmic plasmas the velocity of the charged particles (mechanical velocities) are much slower than the electromagnetic field velocity (speed of light). Therefore, we have:

$$\left[\frac{\mathrm{v}}{c}\right] = [\beta] << 1, \quad [3]$$

which implies that the orders higher than β can be neglected (non relativistic plasma).

From the Faraday equation (second equation of [1]), we can obtain an quantity with dimensions of velocity:

$$[E] = [\mathrm{v}_{el} B], \quad [4]$$

which is the velocity associated to the electromagnetic processes and satisfies the condition:

$$[\mathrm{v}_{el}] \leq [\mathrm{v}]. \quad [5]$$

The last two equations combined give us an estimation of the rate of the electric energy to the magnetic energy:

$$\left[\frac{\varepsilon E^2}{\mu^{-1} B^2}\right] = \left[\frac{E^2}{c^2 B^2}\right] \leq [\beta^2]. \quad [6]$$

If equation [5] is fulfil, the electric component $\rho_E \mathbf{E}$ of the magnetic force that exerts the magnetic field over the plasma is negligible compared with the magnetic component $\mathbf{J} \times \mathbf{B}$.

The displacement current in the Ampère-Maxwell equation (last equation of [1]) is negligible when is compared to the conduction current. The rate of both is given by γ:

$$\gamma = \left[\frac{\omega_{el} \varepsilon}{\sigma}\right], \quad [7]$$

where ω_{el} is the electromagnetic frequency. Taking L as a characteristic length of the electromagnetic and mechanical phenomena (2), we have

$$[\mathrm{v}] = [L \omega], \quad [8]$$

and from [7] we obtain

$$[\omega_{el}] \leq [\omega]. \quad [9]$$

For the Earth's core $\gamma \leq 10^{-18}$ and for stars $\gamma << 1$ (1). The rate of the convection current to the conduction current has the same value γ. From the Gauss law for the electric field (first equation of [1]) we have that $[\rho_E] = [\varepsilon E / L]$, therefore

$$\left[\frac{\rho_E \mathrm{v}}{\sigma E}\right] = \left[\frac{\varepsilon \mathrm{v}}{\sigma L}\right] = [\gamma]. \quad [10]$$

According to equations [7] and [10], equation [2] simplifies to

$$\mathbf{J} = \sigma[\mathbf{E} + \mathbf{v} \times \mathbf{B}]. \quad [11]$$

Thus, the fourth equation of [1] can be written as

$$\nabla \times \mathbf{B} = \mu \mathbf{J} = \mu\sigma[\mathbf{E} + \mathbf{v} \times \mathbf{B}]. \quad [12]$$

To eliminate $\mathbf{E}$, we apply the curl to equation [12] and make the substitution of Faraday's law, yielding

$$\mu\sigma \frac{\partial \mathbf{B}}{\partial t} = \mu\sigma \nabla \times (\mathbf{v} \times \mathbf{B}) - \nabla \times \nabla \times \mathbf{B}. \quad [13]$$

Finally, if we change the second term of the right side with the help of the well known vector identity and use the magnetic Gauss law (third equation of [1]) we arrive to the induction equation

$$\frac{\partial \mathbf{B}}{\partial t} = \nabla \times (\mathbf{v} \times \mathbf{B}) + \eta \nabla^2 \mathbf{B}, \qquad [14]$$

where $\eta = 1/\mu\sigma$ is the magnetic viscosity.

3. Behavior of the induction equation

The rate of the first term on the right side of the induction equation to the second one is given by $R_m = \frac{Lv}{\eta}$, where the adimensional quantity is called the magnetic Reynolds number, in analogy to the Reynolds number for non conducting fluids. The bigger the plasma characteristic lengths is, the bigger the magnetic Reynolds number.

If the first term is much bigger than the second, equation [14] can be written as

$$\frac{\partial \mathbf{B}}{\partial t} = \eta \nabla^2 \mathbf{B}. \qquad [15]$$

This is the diffusion equation, which describes the magnetic field decay in a diffusion characteristic time

$$\tau_\eta = \frac{L^2}{4\pi^2 \eta}, \qquad [16]$$

for a plasma with spherical symmetry. It is of the order of one second for a one centimeter radii copper sphere, 10^4 years for the Earth's nucleus and 10^{10} years for the Sun.

The order of the magnetic Reynolds number can be written as

$$[R_m] = \left[\frac{\omega}{\omega_{el}}\right] = \left[\frac{\tau_\eta}{\tau_0}\right], \qquad [17]$$

where τ_0 is the time associated to plasma mechanical motion. Therefore, for times much slower than the diffusion time the equation simplifies to

$$\frac{\partial \mathbf{B}}{\partial t} = \nabla \times (\mathbf{v} \times \mathbf{B}), \qquad [18]$$

which states that the magnetic flux through any closed curve that moves with the local velocity of the plasma remains constant in time, *i.e.*, the magnetic field lines are dragged by the fluid (*frozen field lines*).

When $R_m >> 1$ the transport of the field lines by the plasma dominates over the diffusion, but if $R_m << 1$ the field decays very fast and the dynamo effect cannot take place. The behavior generated from the interplay of both terms for magnetic Reynolds number values between these limits is very interesting and to explore this is the aim of our work.

4. The induction vector potential

The induction equation [14] can be simplified for the two dimensional case if it is written as a function of the vector potential. We take the magnetic field and the velocity field limited to the *xy* plane, then the magnetic field is obtained from the one component vector potential $\mathbf{A}=A\mathbf{k}$ as follows

$$\mathbf{B} = \nabla \times \mathbf{A} = \left(\frac{\partial A}{\partial y}, -\frac{\partial A}{\partial x}, 0\right), \qquad [19]$$

after the substitution, equation [14] yields

$$\frac{\partial A}{\partial t} = -\mathbf{v} \cdot \nabla A + \eta \nabla^2 A. \qquad [20]$$

We define the position and velocity variables as function of the characteristic parameters (maximum velocity V and maximum length L) as follows

$$v = v' V, \quad x = x' L \qquad [21]$$

with the analogous definition for the y coordinate. The spatial derivatives are given by (similar expressions for the y component)

$$\frac{\partial}{\partial x} = \frac{1}{L}\frac{\partial}{\partial x'} \qquad [22]$$

and

$$\frac{\partial^2}{\partial x^2} = \frac{1}{L^2}\frac{\partial^2}{\partial x'^2}. \qquad [23]$$

After the substitution of these relations and defining the characteristic time of the mechanical motion $\tau_0 = \frac{L}{V}$ (which measures the time it takes the plasma to go from the bottom to the top of the cell), with $t = t'\tau_0$, we obtain

$$\frac{\partial A}{\partial t} = -\mathbf{v}\cdot\nabla A + \frac{1}{R_m}\nabla^2 A, \qquad [24]$$

where the primes have been removed for clarity.

This is the equation we solve under the kinematic condition, *i.e.*, there is no reaction of the magnetic field on the plasma, leaving the velocity field time independent. This approach is valid if the magnetic energy is small compared with the kinetic energy of the plasma, that is

$$\frac{B^2}{8\pi\mu} << \frac{1}{2}\rho_E \mathrm{v}^2. \qquad [25]$$

5. The visualization programs

5.1. Description of the program

We solve equation [24] by using an alternating method in a fourth-order difference schema in a two dimensional cell with perfect conducting upper and lower walls (the magnetic field lines remain always tide to them) and periodic conditions at the lateral walls, *i.e.*, each cell is surrounded by similar cells. The initial magnetic field is homogeneous and points in the y-axis direction.

The velocity field is taken to be incompressible, which allow us to define a stream function from which it can be obtained. We chose the following stream function (figure 1) shown in the figure 1

$$y = -\frac{1}{4\pi}\left[4(1-m)\left(x-\frac{1}{2}\right)^2 - m\right]\left[1-4\left(y-\frac{1}{2}\right)^2\right]^4 \cos\left[\pi\left(x-\frac{1}{2}\right)\right], \qquad [26]$$

with ($0 \le x \le 1$, $0 \le y \le 1$), m is an adjustable parameter ($0 \le m \le 1$) that allow us to select different velocity fields. When m=1 it describes a single eddy, as m decreases two new symmetrical eddies emerge from each side compressing the original eddie. At one point, there are three eddies, but as m gets closer to zero, the central eddy disappears and just two eddies remain, rotating in same directions (figure 1a).

Time is measure in $\tau_0 = \frac{L}{V}$ units; where V and L are the characteristic plasma velocity and the characteristic length of the cell. For granules, mesogranules and supergranules the values V=900, 60 and 400 m/s and L=1.4×10^3, 7×10^3 and 3×10^3 km, respectively, yields τ_0 values of 26 minutes, 1.35 days and 0.87 days (12, 13).

The magnetic Reynolds number is given as an input parameter. For laboratory plasmas is low due to small scales and slow plasma velocities. To study supergranules the highest Reynolds number allows by the program should be used ($R_m = 1000$).

5.2. PCell and XPCell

The user, who desires to run the PCell and XPCell under Linux, needs the following free programs:

– XFORMS

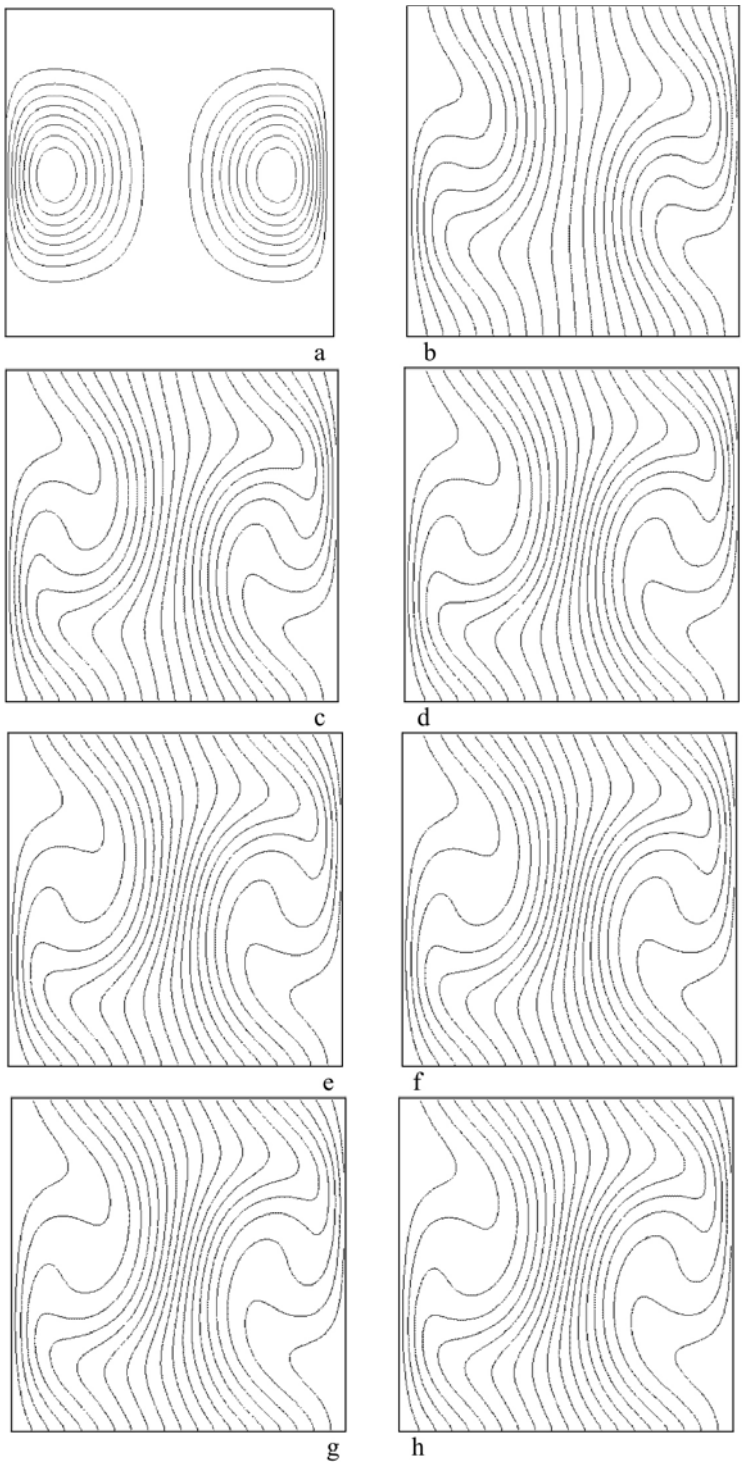

Figure 1. The stream function for m=0.005 (a) and the corresponding time evolution of the magnetic field with R_m = 500 (b-h) at different times. At the beginning the magnetic field is oriented on the y axis. In this case, the steady state is reached quickly (c-h).

– GNUPLOT

– OpenGL

These programs are available for allmost all computer systems. The XFORMS library was used to design the control panel. Both programs use the same control panel. The data generated by PCell is processed by GNUPLOT to produce the simulation. The user can create movies with both versions. With PCell the movie format is MPEG.

The new version, XPCell uses OpenGL for the visualization, so the visualization is displayed in a square window, while the one provided by GNUPLOT in PCell is not. For more information about the program, the interested user may visit the website, we mentioned above.

XPCell uses CONREC, a contouring program written by Paul D. Bourke. For more information about this routine, the interested reader may consult following Webpage: http://local.wasp.uwa.edu.au/pbourke/papers/conrec/

5.2.1. The control panel

When the program starts, it creates a window: the *Plasma Cell Control Panel*. The user can control all items on it interactively with the mouse. The control panel has the following items (figure 2):

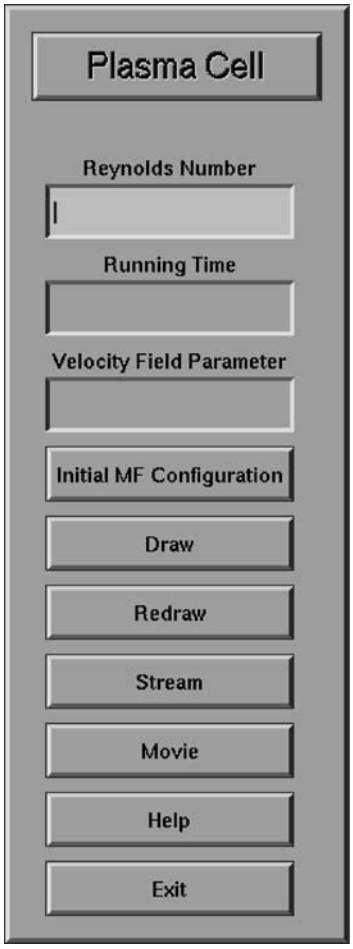

Figure 2. PCell and XPCell Control Panel.

– The velocity field parameter input: The user chooses the velocity field selecting a value of the m parameter ($0 \leq m \leq 1$).

– The magnetic Reynolds number input: The user enters the magnetic Reynolds number ($0 < R_m \leq 1000$).

– The running time input: The user enters this time in units of $\tau_0 = \frac{L}{V}$. The values of V and L are chosen equal to one, thus the magnetic Reynolds number $R_m = \frac{LV}{\eta}$ equals the reciprocal viscosity. At this time, the program stops.

– Initial MF (Magnetic Field) Configuration: Not yet implemented.

– The Draw button: This button starts the program that calculates the magnetic field at each time interval (these data is stored in the files `pcell1.dat`, `pcell2.dat` and so on) and after a short time, when the generation of data is finished, the display window opens (figure 3).

– The Redraw Button: To display the simulation of previously obtained data, to avoid repeating an already existing calculation. It applies only for `pcell`.

– The Stream button: Displays the mechanical motion of plasma (figure 1a).

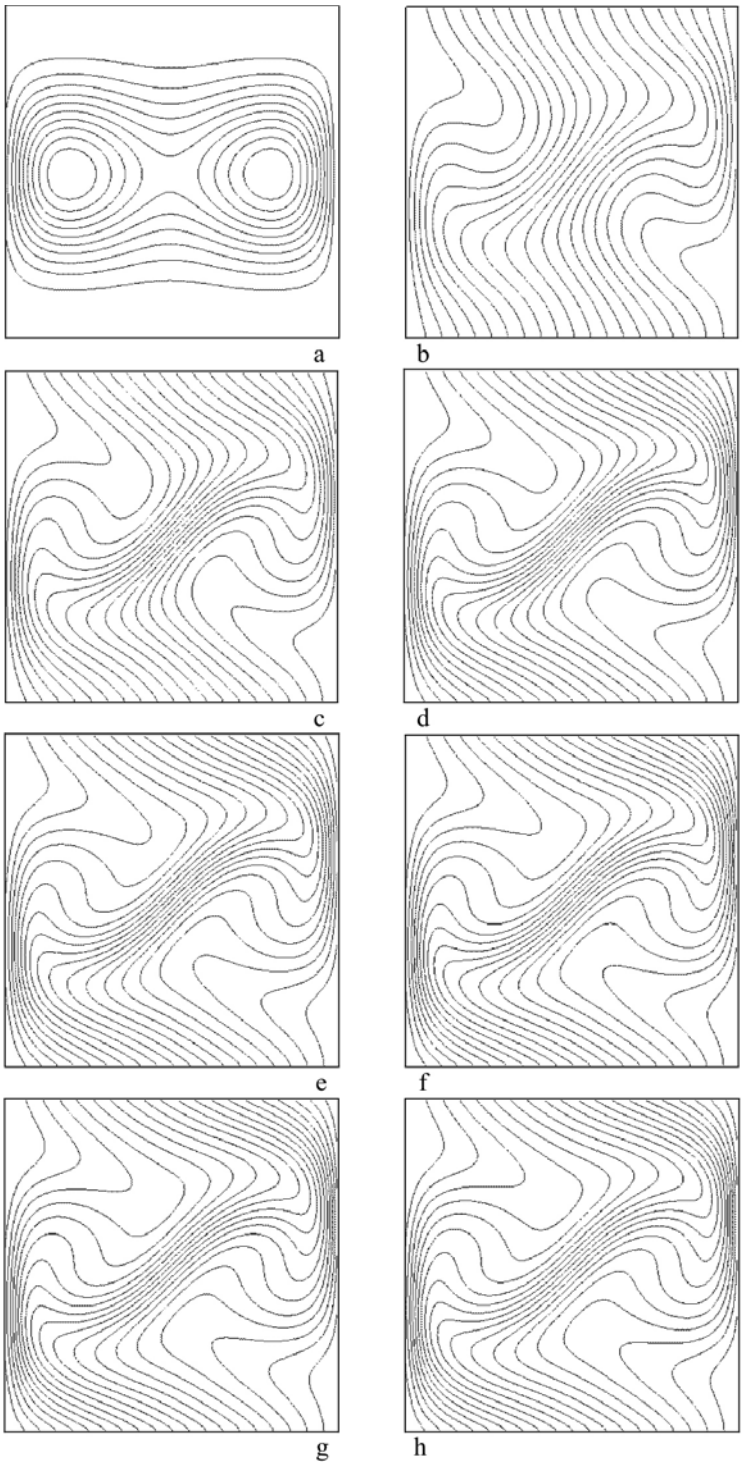

Figure 3. The stream function for m=0.15 (a) and the corresponding time evolution of the magnetic field with R_m = 500 (b-h) at different times. At the beginning the magnetic field is oriented on the y axis. In this case, the steady state is reached quickly (f-h).

– The Movie button: The users can create their own movies and display them with a MPEG player. The name of the created movie is `convection.mpg` for `pcell` and `convection.avi` for `xpcell`.

– The Help button: Not yet implemented.

– The Exit button: To leave the session. If the user wants to remove all `pcell*.dat` then type `rm -rf pcell*.dat` on the prompt (it applies only for `pcell`).

The magnetic Reynolds number, the running time, and the velocity field parameter inputs can be used in any order, but the user should enter values before any other item of the program (Draw, Redraw, Stream, Movie). The evolution of the magnetic field lines are displayed on a new window (GNUPLOT or OpenGL). When a given velocity field is selected it is shown here too. For for XPCell an OpenGL Window appears immediately. For PCell the GNUPLOT windows appears but after all data file were created.

6. Applications

There are some interesting applications that the user can explore. Among these are (figures 1 and 3):

– The evolution of the magnetic field lines as function of the magnetic Reynolds number.

– The mechanism of magnetic field dissipation and the reconnection phenomena.

– The evolution of the averaged magnetic density as function of the magnetic Reynolds number.

– The maximum averaged magnetic density as function of the magnetic Reynolds number.

– The stationary state of the averaged magnetic density and the way it is reached as function of the magnetic Reynolds number.

– The time it takes to reach the maximum and the stationary state of the averaged magnetic density as function of the magnetic Reynolds number.

6.1. Evolution of the magnetic field

The stream function and the magnetic field twist evolution can be visualized easily with PCell and XPCell. In figures 1 and 3-7 illustrations of this evolution can be seen.

Magnetic reconnection of the magnetic field lines is one of the mechanisms responsible for solar flares and other plasma phenomena. These magnetic reconnections appear in figure 4-7.

6.2. Analysis of the magnetic field evolution

For high Reynolds numbers the convection generates a magnetic field component parallel to the plasma motion. The field begins to amplify itself, becoming stronger at the lateral borders of the cell (figure 3-4, and 6-7). As this happens the spatial scale, where the variation of the field occurs, decreases linearly, producing an increase of the diffusion. When this resistive term becomes of the same order as the convective term the amplification of the field stops. Therefore, the averaged magnetic density reaches a maximum (figure 8). The twisting of the field produces regions of high magnetic density at the same time that the diffusive term becomes bigger and reconnection of the magnetic filed lines occur expelling the field from the central region of the eddy, reaching the magnetic density a stationary value (figure 1 and 3). This stationary value is independent of the velocity field but the way it is reached depends on the velocity field (figure 8).

For velocity fields dominated by one eddy the magnetic energy in the central part of the cell is very small compared with the density at the borders, as the field is ex-

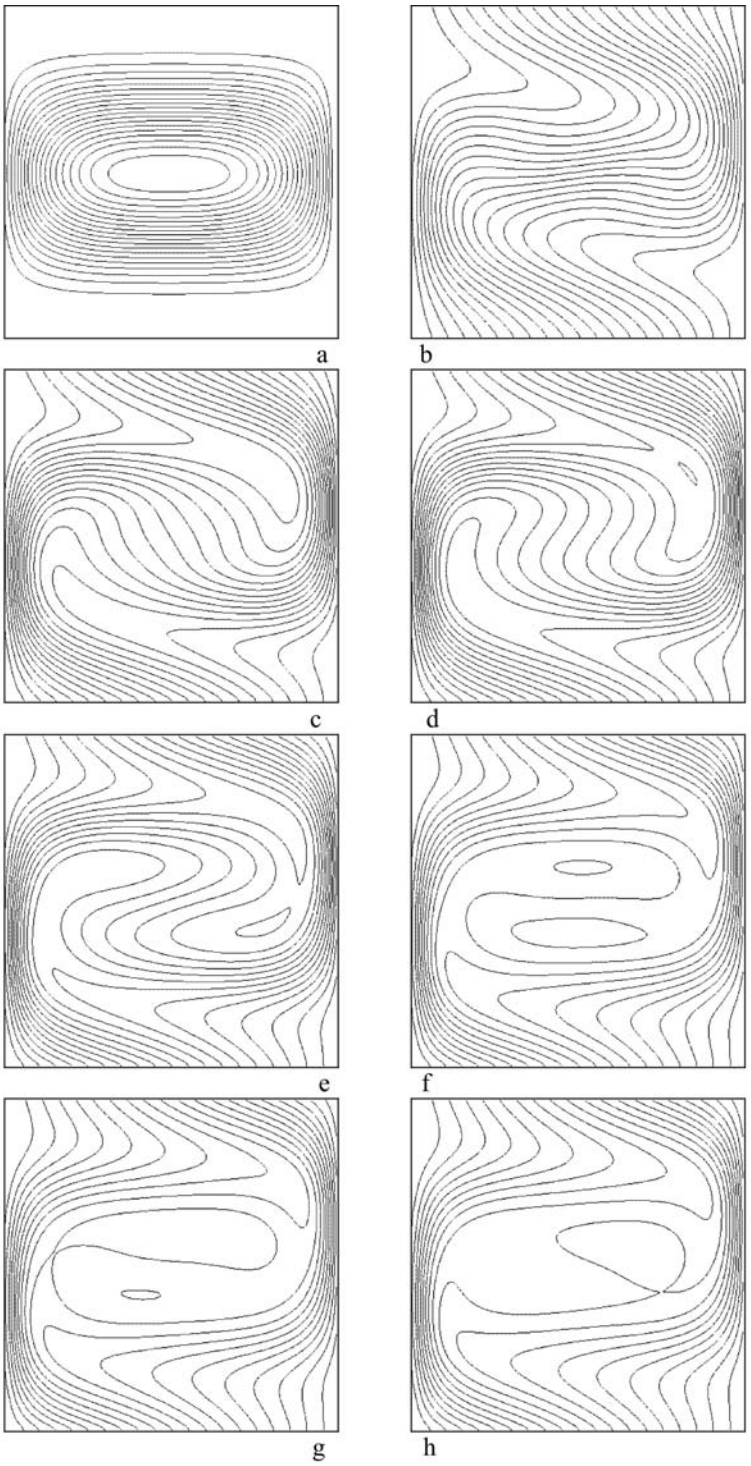

Figure 4. The stream function for m=0.5 (a) and the corresponding time evolution of the magnetic field with R_m = 500 (b-f) at different times. Magnetic reconnections appear in (c-h). At the beginning the magnetic field is oriented on the y axis.

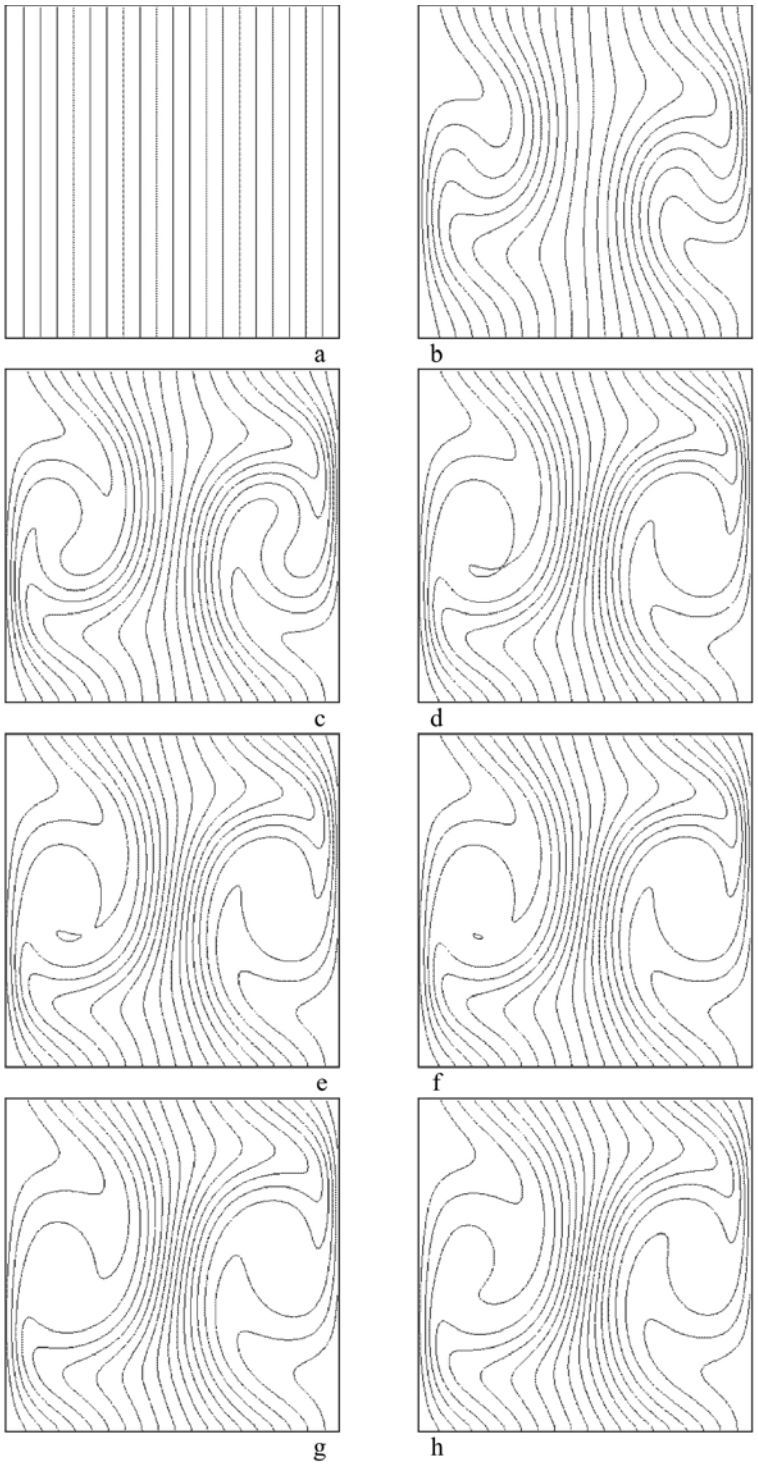

Figure 5. Time evolution of the magnetic field for R_m = 1000 (a-h) at different times. At the beginning the magnetic field is oriented on the y axis (a). The stream function (m=0.005) appears in frame (a) of figure 2. Magnetic reconnections appears in frames (d-f).

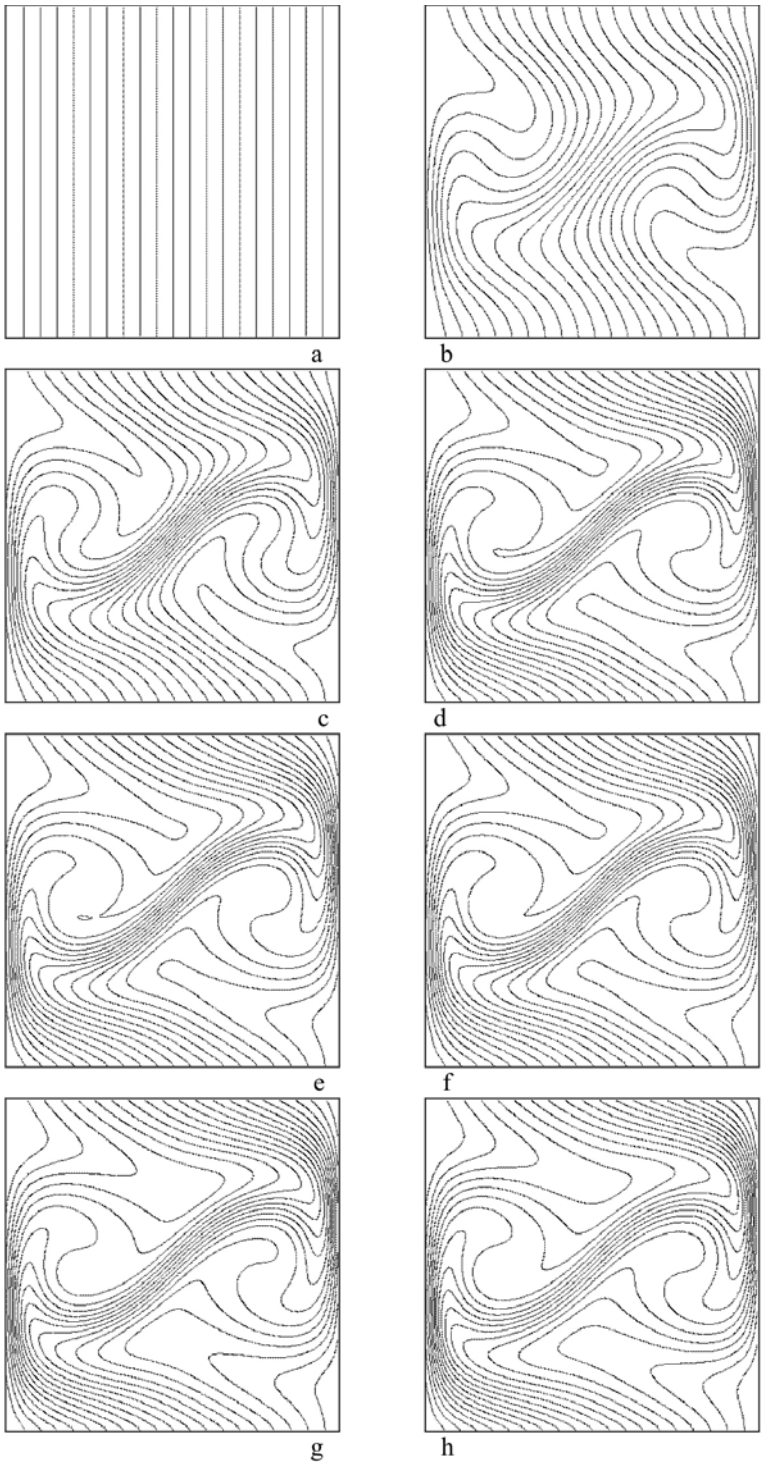

Figure 6. The time evolution of the magnetic field for R_m = 1000 (a-h) at different times. At the beginning the magnetic field is oriented on the y axis (a). The stream function (m=0.15) appears in frame (a) of figure 3. Magnetic reconnections appear in frames (d-e).

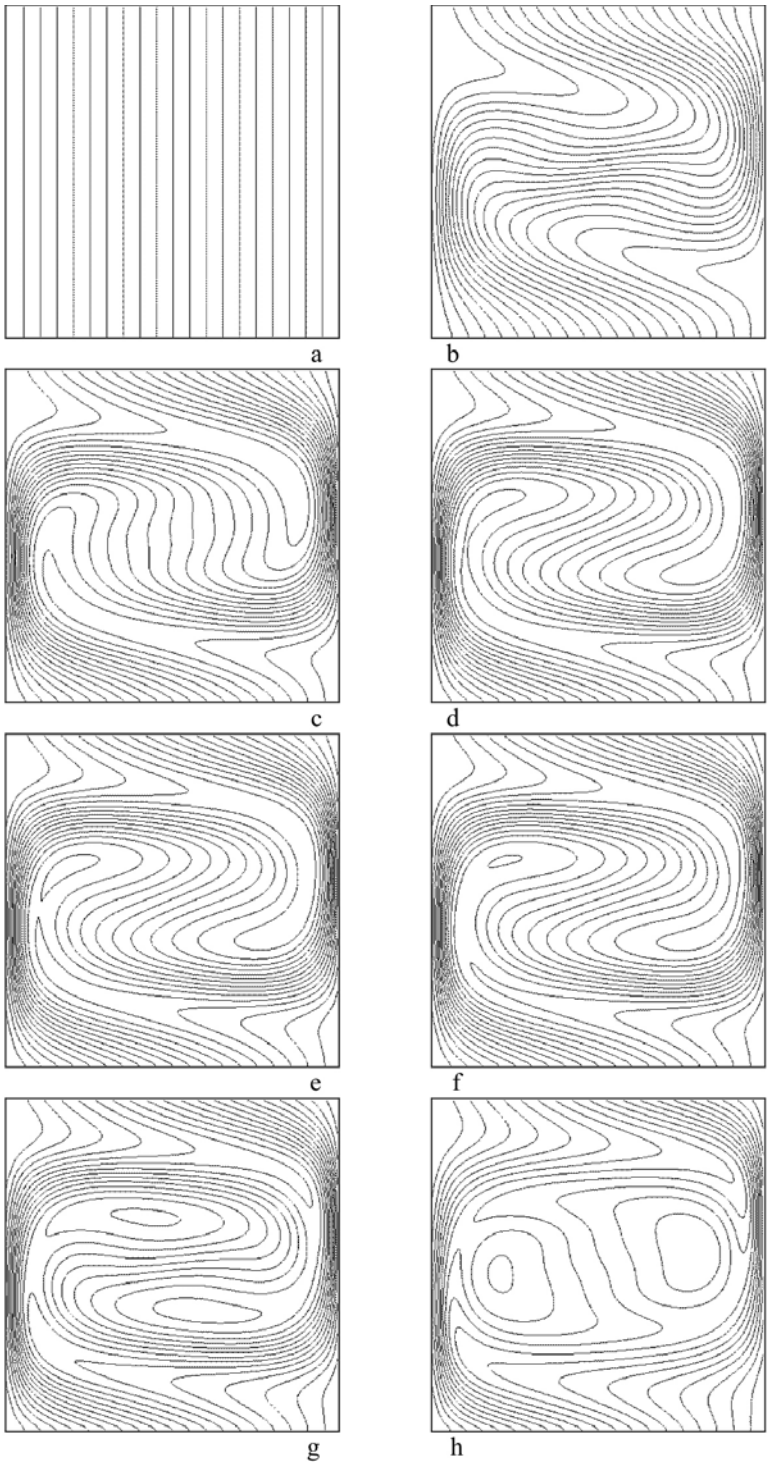

Figure 7. The time evolution of the magnetic field with R_m = 1000 (a-h) at times. At the beginning the magnetic field is oriented on the *y* axis (a). The stream function (*m*=0.5) appears in frame (a) of figure 4. Magnetic reconnections appear in frames (d-h).

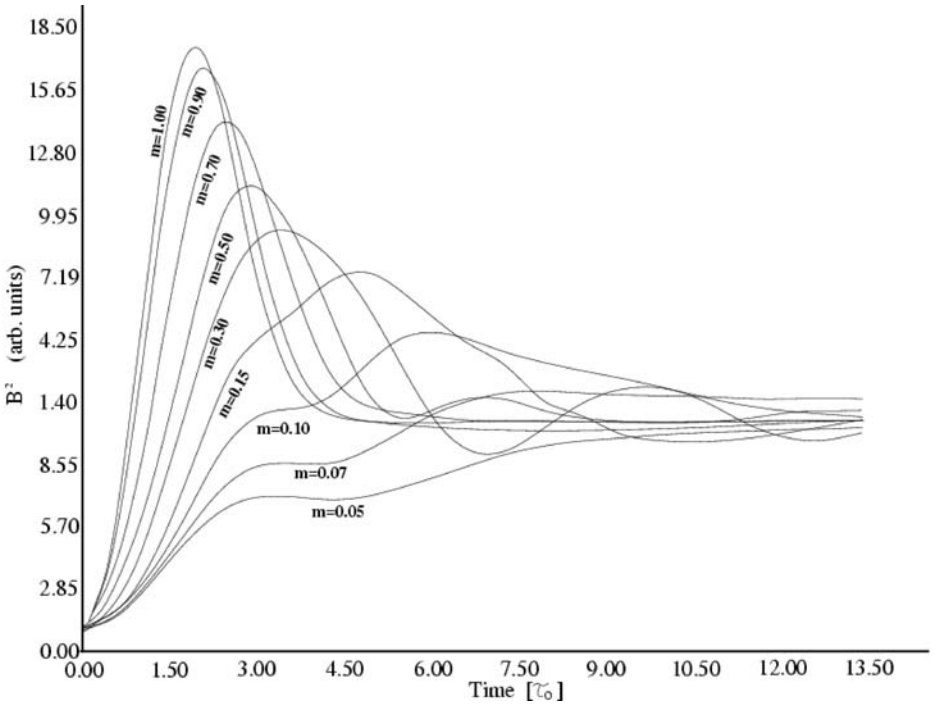

Figure 8. Square of magnetic field as a function of time for different *m* values.

pelled from the central part by the diffusion the magnetic density does not change much so the stationary value comes from the field located at the borders. For velocity fields with a strong influence of lateral eddies an additional region of high magnetic density appears in the middle of the cell, where the central eddy is located (figure 6). The intensity of the field is of the same order as the one at the borders; the twisting of the field as it disappears on both sides of the central region of high density makes the average magnetic density oscillate until it reaches the stationary value. When the velocity fields are practically two eddies (small *m*) the magnetic field at the borders is not very strong and the generation of the central high density zone helps to reach the maximum value, which is the same as the stationary one (figure 8).

It is importance that the average lifetime of the granules and mesogranules are very small compare to the characteristic time ($\sim 0.31\tau_0$ and $\sim 0.07\tau_0$, respectively). Therefore, for these motions the behavior shown would not evolve because the structures have disappeared long before. On the other hand, in supergranules ($\sim 23\tau_0$) the stationary state is reached.

According to the above description for single eddies, a simple expression for the maximum averaged energy density and the Reynolds number can be obtained: $B^2_{\max} = R^{2/3} B^2_0$, where B_0 is the initial averaged magnetic field (2, 8). In figure 9a it can be seen that this behavior is still valid for plasmas with interacting eddies. The Reynolds number exponents obtained for the values of m=1.0, 0.7, 0.3, 0.1 are respectively 0.59, 0.55, 0.54, 0.67. In the same way a relation between the stationary averaged energy density is obtained (2, 8): $B^2_{st} = R^{1/2} B^2_0$. Figure 9b shows the result of the simulations which agree very well with this relation even for interacting eddies. The Reynolds number exponents obtained in this case are 0.42, 0.42, 0.43, 0.48 in the same order as above.

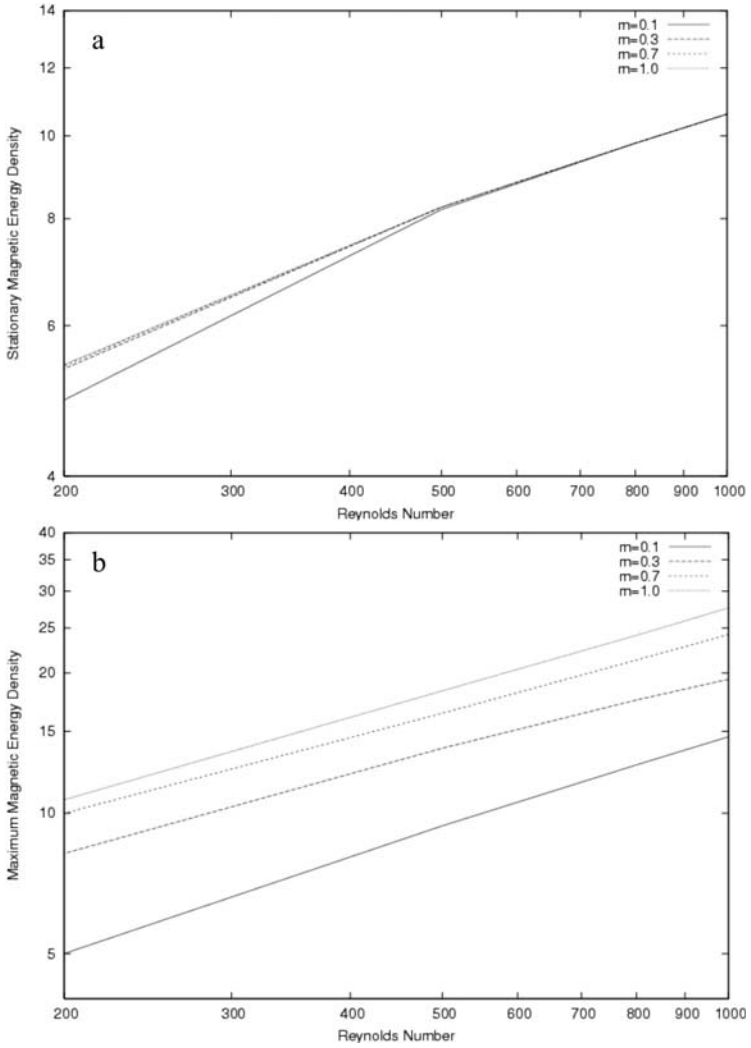

Figure 9. Stationary (a) and maximum magnetic energy density (b) as function of the magnetic Reynolds number for different *m* values.

7. Conclusions and future work

The kinematical dynamo model presented here produces intensification of the magnetic field by the induction of plasma trying to move across field lines in regions of small eddies between big convective zones, in addition to the usual one accumulated on the regions between cells. Although this model does not include the feedback of the force on the inducting motion and has no rotation profile, the generation of a toroidal field is clear. Similar oscillatory behavior of the magnetic field for bands of asymmetrical eddies has been found for groups of four-cell convections by Zegeling (14) working on the same principle here described.

The model could be implemented to solve the full dynamo problem, which involves the simultaneous solution of the induction equation, along with the equations of motion, continuity and thermodynamics. The inclusion of the term produces the freezing of the magnetic field to the electron flow instead to the bulk velocity field (8).

Implementations of the numerical methods will allow us to expand the study, including the effects of nonlinearity and chaotic motion at Reynolds numbers typical of astrophysical problems, where self organization emerges (15, 16).

New approaches have been developed to calculate in a more efficient way convective cells. One strategy is the adaptive grid method, which based on a coordinate transformations between physical and computation coordinates, automatically track and spatially resolve nonlinear structures (17).

As a didactical tool, a program to visualize the magnetic field in a plasma confined to a cell is very useful, especially if the user can create movies by changing the parameters involved in the induction equation. The versatile program we have described functions quickly and interactively with the keyboard and the mouse, but there is room for improvement.

Future work

The program can be improved in the following way:

- Including more velocity fields.
- Adding the magnetic density averaged over the cell, represented as function of time.
- Expanding to three dimensional cells and using other shapes like hexagonal cells (this shape appears as stable patterns in some fluids).
- Considering mechanical-electromagnetic interaction between the plasma and the field.
- Exploring more complex behaviors such as Chaos.

Acknowledgment

The authors would like to thank Dr. rer. nat. Jorge Páez for helpful comments.

References

1. DOLGINOV A.Z. ***Phys Reports*** 162: 337-415.1988.
2. ELSASSER W.M. ***Rev Mod Phys*** 28 (2):135-163. 1956.
3. WEISS N.O. ***Proc Roy Soc*** 293: 310-328. 1966.
4. PARKER E.N. ***Astrophys J*** 138: 552-562. 1975.
5. WEISS N.O. ***Adv Chem Phys*** 32: 101-110.1975.
6. GALLOWAY P.A., PROCTOR M. R.E., WEISS N.O. ***J Fluid Mech*** 87: 243-254. 1978.
7. GALLOWAY P.A., WEISS N.O. ***Astrophys J*** 243:120-130. 1981.
8. MININNI P. D., GOMEZ D.O., MAHAJAN S.M. ***Astrophys J*** 587: 472-481. 2003.
9. CARBONI R. Convective Plasmas (To obtain de M. Sc. in Physics). School of Physics. University of Costa Rica. San José (Costa Rica). 154pp. 1994.
10. CARBONI R., FRUTOS-ALFARO F. ***Comp Sci and Eng*** 2-5: July/August. 2004.
11. CARBONI R., FRUTOS-ALFARO F. ***J Atmos and Sol-Terr Phys*** 67: 1809-1814. 2005.
12. FOUKAL P. ***Solar Astrophysics.*** Wiley & Sons. New York. 1990.
13. STURROCK P.A., T. HOLZER T., MIHALAS D.M., ULRICH R.K. (Editors) ***Physics of the Sun.*** Reidel. Dordrecht. 1986.
14. ZEGELING P.A. ***J Sci Computing.*** Special ICIAM issue. 2005.
15. CHANG T., TAM S.W.Y.,WU C. ***Phys Plasmas*** 11: 1287-1299. 2004.
16. VALDIVIA J.A., KLIMAS A., VASSILIADIS D., URITSKY V., TAKALO J. ***Space Sci Rev*** 107:515-522, 2003.
17. ZEGELING P.A., KEPPENS R. ***Adaptive Method of Lines*** (Eds. Vande Wouwer A., Saucez Ph., Schiesser W.E.) Chapman & Hall/CRC. 2001.